

Electromagnetic Modeling and Design of Haptic Interface Prototypes Based on Magnetorheological Fluids

R. Rizzo^{1,2}, N. Sgambelluri², E. P. Scilingo², M. Raugi¹, and A. Bicchi², *Fellow, IEEE*

¹Department of Electrical Systems and Automation, University of Pisa, 56100 Pisa, Italy

²Interdepartmental Research Center "E. Piaggio," University of Pisa, 56100 Pisa, Italy

We report on the design and implementation of innovative haptic interfaces based on magnetorheological fluids (MRFs). We developed 2-D and quasi-3-D MRF-based devices capable of suitably energizing fluids with a magnetic field in order to build shapes that can be directly felt and explored by hand. We obtained this effect by properly creating a distribution of a magnetic field over time and space inducing the fluid to assume a desired shape and compliance. We implemented different prototypes, synthesized and designed with the help of preliminary simulations by a 3-D finite-element code. In this way, both magnetic field and shear stress profiles inside the fluid could be carefully predicted. Finally, we evaluated and experimentally assessed the performance of these devices.

Index Terms—Electromagnetic devices, haptic interfaces, magnetorheological fluid (MRF).

I. INTRODUCTION

HAPTIC information is a relevant and essential cue when interacting with simulated objects in virtual environments. Indeed, haptics deal with the sense of touch and study the use of touch sensation in order to produce computer interfaces that allow users to interact with virtual objects by means of force feedback and tactile feedback. The primary application field for haptic interfaces and displays is to provide a realistic sense of physics to the users immersed into a virtual world. An ideal haptic display should provide a convincing "immersive" sensation to the user of being "in touch" with a remote or virtual world. The quality of the virtual presence is often negatively affected by perceptual artifacts generated by wearing heavy and/or cumbersome exoskeletons or rigid linkages. When tactile perception is mediated by instruments or rigid devices, the sense of touch is affected as a consequence of the poorer dynamics and control of manipulation. Authors have already investigated the possibility of using magnetorheological fluids (MRF) in haptic interfaces, exploiting their property of changing the rheological behavior by tuning an external magnetic field. Unlike kinaesthetic displays present in literature, we proposed a MRF-based system that allows a direct contact with a compliant object. In this way both kinaesthetic and cutaneous channels of the fingerpads are stimulated during manipulation, and tactile perception is involved in all its components. The MRF-based haptic display is based on a freehand concept, in which users can put their hand within a box and freely interact with the suitably controlled fluid. The magnetic field is produced by solenoids properly placed to provide a homogeneous distribution throughout the fluid. The system must be according to electromagnetic synthesis criteria, i.e., focusing the magnetic flux into specific regions of the MR fluid, permitting to build figures with a given shape and compliance. A suitable control strategy should be implemented to drive the MR fluid in order to mimic a wide range of rheological behaviors, within limits dictated by saturation effects in the fluid. Nevertheless, other

possible configurations, including mechanical arrangements, could be considered in future developments as well.

All the devices here described are composed by a configuration of ferromagnetic cores suitably contoured in order to form the interface between the device and MR fluid. Adapted main design criteria are low reluctance flux paths, uniformity of the magnetic field in the interest region, and accessibility of the MRF by the user.

Since the behavior of both MR fluid and ferromagnetic cores is highly nonlinear, an analytical method cannot perform an accurate analysis of the proposed system. In order to take into account the $B-H$ function for nonlinear materials, the leakage flux due to different magnetic path in air, as well as the presence of different feeding coils, the simulations of the present work have been carried out by the use of a 3-D finite-element code [1] briefly described in the Appendix.

II. MRF-BASED HAPTIC INTERFACES

Typically, a haptic device is placed inside a loop, where a human operator tactually interacts with a virtual environment. The device senses motion and force on the end-effector, or handle, and produces a force feedback sensation.

Touch macroscopically involves kinaesthetic perception mediated by the positions and forces at the finger articulations, while microscopically it induces a cutaneous sensation through the mechanoreceptors lying in the skin [2].

Although it is widely acknowledged in the neuroscience and psychophysics literature [3], [4] that information from cutaneous receptors in the hand is quite important in tactile interaction, most present-day haptic displays are limited to kinaesthesia.

Analogously to the hand, artificial devices should replicate these perceptual channels [5]. While kinaesthetic information is satisfactorily replicated by current technology, cutaneous information is still a challenging goal to be attained: the realization of sensors and displays that have comparable resolution with that of human apparatus of cutaneous receptors is a formidable task for today's technology.

In order to address such multichannel tactile perception, innovative solutions are needed. The aim of this study is to develop unconventional haptic electromagnetic systems to mimic

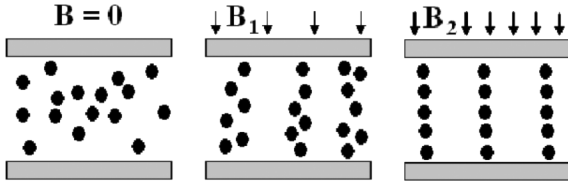


Fig. 1. Schematic view of the operation of the MRF.

the behavior of some viscoelastic materials by using “smart materials” such as MRF.

Our research consists of developing devices, as nonimmersive and/or immersive free-hand configurations, exploiting rheological properties of MRF, modulated by properly acting on magnetic fields in a controlled volume.

A. Magnetorheological Fluids

Magnetorheological fluids, also termed controllable fluids, are a particular class of smart materials, capable of changing their rheological behavior when an external magnetic field is applied [6]–[8]. Such fluids are synthetic oil-based or water-based suspensions of magnetically polarizable particles (size 0.05–1 μm) and exhibit a rapid, reversible and tunable transition from a liquid to a near-solid state upon the application of an external magnetic field. Typically, this change is manifested by the development of a yield/shear stress that monotonically increases with the applied field. Just as quickly, the fluid can be returned to its liquid state by removing the magnetic field, being the phenomenon reversible [9]–[11].

In order to describe this mechanism, we consider a MRF located in a gap created between two plates as shown in Fig. 1. In the absence of an applied magnetic field, the fluid flows freely through the gap being the polarizable particles randomly distributed in the fluid. The application of an external magnetic field develops a precisely controllable yield/shear stress in the fluid: the polarizable particles within the gap align themselves in the same direction of the field creating particle chains and restricting the movement of the fluid. The degree of change in terms of yield/shear stress is nearly proportional to the magnitude of the magnetic field. Since the rheological behavior and the mechanism used to activate the MRFs depend on the temperature, their operating range is approximately -40°C to 150°C . In terms of their consistency or softness, controllable fluids appear liquid in the off-state, exhibiting a viscosity ranging from 0.20 to 0.30 Pa·s at 25°C . When a magnetic field is applied, the fluid turns from liquid to near solid in few milliseconds by changing significantly its apparent viscosity. When a saturation magnetic field is applied, approximately in 10 ms MRFs exhibit a typical level of saturation yield/shear strength up to 100 kPa.

Their application field is typically related to devices such as valves, brakes, clutches, and dampers, in civil and electro-mechanical engineering applications [6], [10], [12]–[16]. Rheological fluids are commonly used in the field of vibration control, in automotive applications [17], [18], and the aerospace industry [19]–[23].

From a physical point of view, the MR fluids exhibit their rheological behavior operating in “shear,” “flow,” or “squeeze” mode. As shown in Fig. 2, the fluid is deformed in a direction

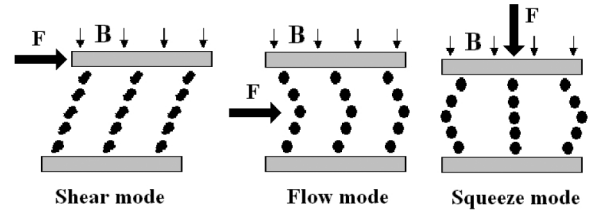


Fig. 2. Modes of mechanical stress of a MRF.

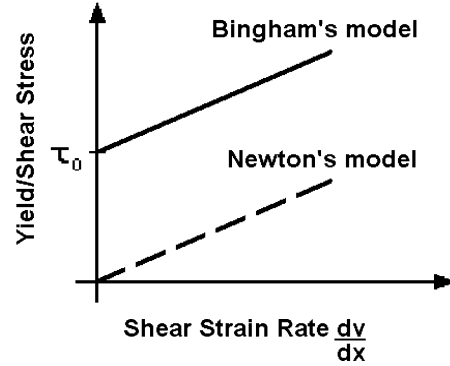


Fig. 3. Simplified model of the MRF.

approximately orthogonal to the arrays of particle chains in the shear and flow mode. Instead, it is subjected to compressive and tensile stresses in a direction parallel to the chains in the squeeze mode [10]. Although many common applications employ the MRF in a single mode, in our application the complete manipulation of a virtual object, reproduced on the MRF volume, is the sum of the shear, flow, and squeeze modes. However, for all the used modes, the electromechanical parameter of interest is the yield/shear stress $\tau = \tau(B)$ that indicates the transition between a Newtonian-like and a Bingham-like behavior, that is, between the liquid to the semi-solid state. A very simplified model of such fluids is shown in Fig. 3 and is described by the following equations:

$$\begin{cases} \frac{dv}{dx} = 0, & \text{if } \tau < \tau_0(B) \\ \tau = \tau_0(B) + \eta \frac{dv}{dx}, & \text{if } \tau \geq \tau_0(B) \end{cases}$$

where $\tau_0(B)$ is the yield/shear stress as a function of the flux density, η is the viscosity, and dv/dx is the fluid shear rate.

When $\tau < \tau_0(B)$, the fluid shear rate is null ($dv/dx = 0$) and the MRF has a semi-solid behavior. On the contrary, if $\tau \geq \tau_0(B)$, the fluid shear rate $dv/dx \neq 0$ and the fluid begins its transition towards a liquid state.

In our applications, we used a commercial magnetorheological fluid marked MRF132LD produced by Lord Corporation, Cary, NC. The main magnetic and rheological characteristics of this fluid are shown in Fig. 4 and can be synthesized as follows.

Magnetic properties:

- Saturation threshold: $B_s \cong 0.5 - 0.6 \text{ T}$;
- Relative initial permeability: $\mu_{r_initial} \cong 3.5$;
- Maximum relative permeability: $\mu_{r_max} \cong 7.4$.

Mechanical and rheological properties:

- Response time: $t_{on} \cong 10 \text{ ms}$;
- Maximum yield/shear stress: $\tau_{max} \cong 55 \text{ kPa}$.

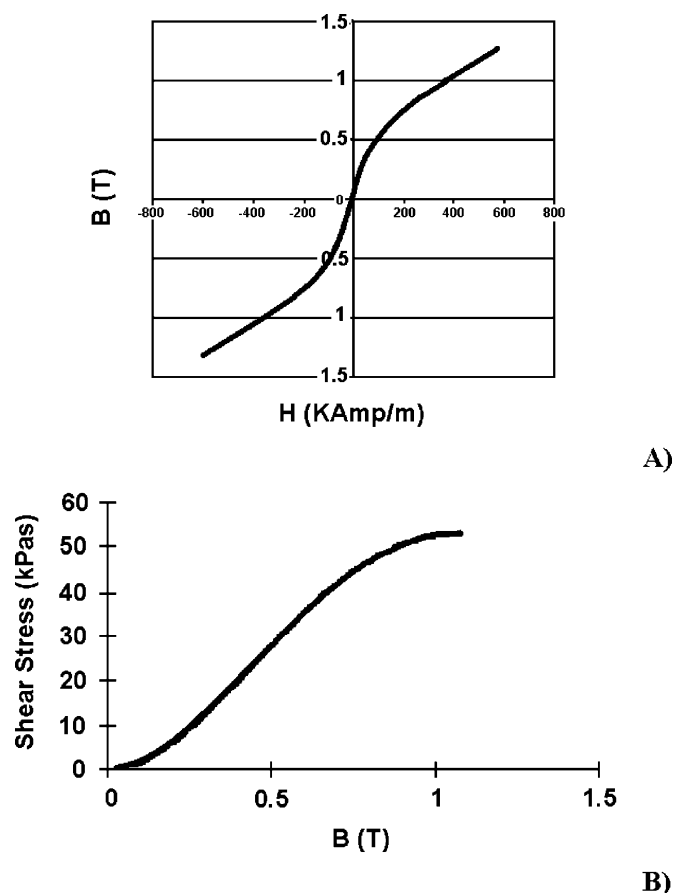


Fig. 4. Magnetic (A) and rheological properties (B) of MRF132LD.

By using the characteristics of the selected fluid, we can evaluate the operating point of the MRF and consequently the magnetic field B able to determine the desired yield/shear stress τ_0 .

B. State-of-the-Art and Innovative Solutions

Conventional haptic devices are based on conventional electromechanical devices (e.g., PHANTOM by SensAble, Delta by Force Dimension) that provide force and torque at an interface (e.g., a stick or a thimble) with a human operator. Although such devices (e.g., [24], [25]) are able to provide good replication of kinaesthetic cues, they cannot address the cutaneous system of receptors and present a somewhat artificial, encumbering interface to the human.

The use of smart fluids for the development of haptic devices could be an alternative solution. The advantage of using controllable fluids is the possibility to design and realize a variety of real applications by using semi-active controls without additional mechanical parts [26]–[28]. On the other hand, the effects of rheological fluids can be combined with other actuators such as electromagnetic, pneumatic, or electrochemical actuators so that novel, hybrid actuators are produced following high-power density and low-energy requirements [29]–[32].

Although some authors [33]–[38] have already explored the possibility of using rheological fluids in tactile displays, their attention has been focused on the use of different smart materials that change their rheology by applying an electric

field (electrorheological fluids—ERFs). A prototype based on ERF for blind people is a tactile graphic I/O tablet [38]. Another example conceived for medical teleoperation systems is the MEMICA glove, whose components are miniature electrical actuators based on the ERFs [39]. Since ERFs exhibit a maximum level of saturation yield strength of about 5 kPa with a typical response time of about 100–200 ms, it is unusable for our purposes. Furthermore, another serious drawback associated with the ERFs is the relatively large exciting voltage (typically up to 10 kV) that not allows the operator to come into direct contact with the fluid.

Concerning MRFs, at present the only known developed device for medical application based on MRFs is a portable hand and wrist rehabilitation device [40]. This device includes a small, hand-held housing for a magnetic fluid controllable resistance brake. Although it is based on MRFs, our technological approach is completely different, because our devices allow a direct contact of the operator with the fluid.

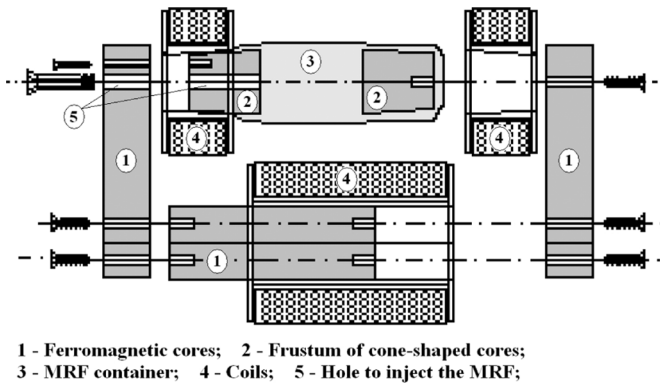
In order to develop an innovative haptic interface, we envisioned two possible schemes for MRF-based displays. In the first one, the Pinch Grasp (PG) device, the MRF specimen is positioned in the air gap of an electromagnet allowing pinch grasp manipulation. In the second scheme, the Haptic Black Box (HBB), a given volume of MRF is placed into a plastic box into which a hand can be introduced to freely interact with the fluid. Both configurations were designed to focus a magnetic flux into a specified region of the MRF, maximizing the magnetic field energy in this region and minimizing the energy lost in the other regions. An accurate magnetic field profiling permits to build figures with a given shape and compliance.

1) *A First Preliminary Prototype: The Pinch Grasp (PG)*: The Pinch Grasp was built in order to verify the ability of using MRFs to mimic the compliance, damping, and creep of some materials, reproducing virtual object softness.

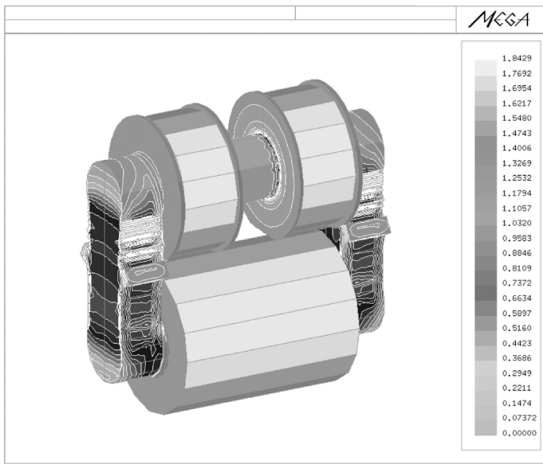
The device, shown in Fig. 5, consists of a ferromagnetic core of “AISI 1015” steel and three coils driven by a total dc supply of 5000 A. Two pieces of the core take the shape of a frustum of cone in order to facilitate the connection between the core itself and the container of the MR fluid. Two coils are made up of a bundle of 1200 filament wires fed by a current of 1 A. The third coil, mounted on the down yoke, consists of 1500 filament wires with a current of 1.7 A. These currents have been chosen to obtain a value of B inside the MR fluid around 0.55 T, under continuous operating conditions. The fluid container consists of a small balloon embedded between the cores and the coil support. When the whole system is mounted, the fluid is injected through a hole in the core filling the container to form the specimen.

As a first application, the PG device was used to develop a mechanical model of the fluid, submitting the MRF specimen to a *stress relaxation* test by using the experimental setup shown in Fig. 6.

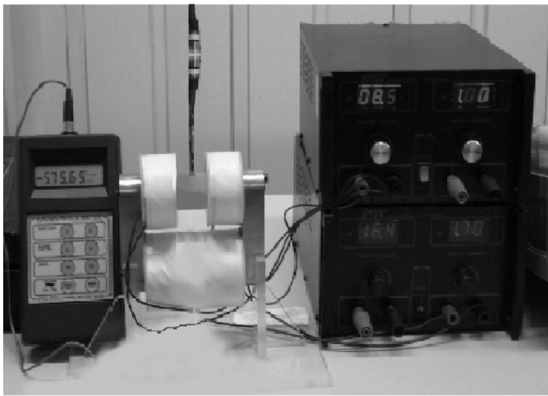
Experiments were carried out applying stepwise strains to the MRF specimen exposed to increasing magnetic fields and acquiring the relative stress relaxation curves. Tests were repeatedly performed in order to reject the hypothesis of statistical randomness. The strain imposed was 10%, while the application time (about 10 s) was chosen to be greater than the decay time of the phenomenon. The magnetic field incremental step



A)



B)



C)

Fig. 5. Pinch Grasp. (A) Schematic view of the device. (B) FE simulation. (C) Prototype.

was equal to $\Delta B = 0.03125$ T, corresponding to an increment of the coil current of 0.05 A. In Fig. 7, stress relaxation curves as a function of magnetic fields are reported. It is worthwhile noting that the force ranges from a few thousandths *N* in the absence of a magnetic field to about 1.4 N when the MRF phenomenon is already saturated. Furthermore, for magnetic fields greater than 0.55 T, the MRF specimen does not show significant stress relaxation. For this reason, the magnetic field range was restricted to $0 \div 0.55$ T, where differences in the fluid behavior are more pronounced. Analyzing the profile of the curves reported in Fig. 7, after an initial peak, the stress curve relaxes

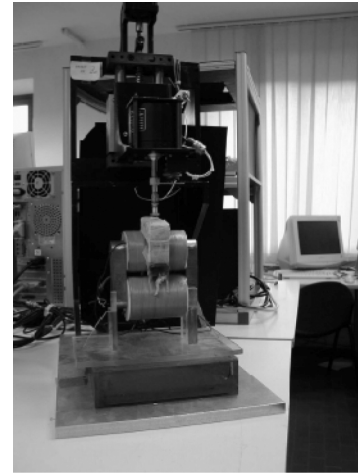


Fig. 6. Experimental apparatus used to identify the MRF.

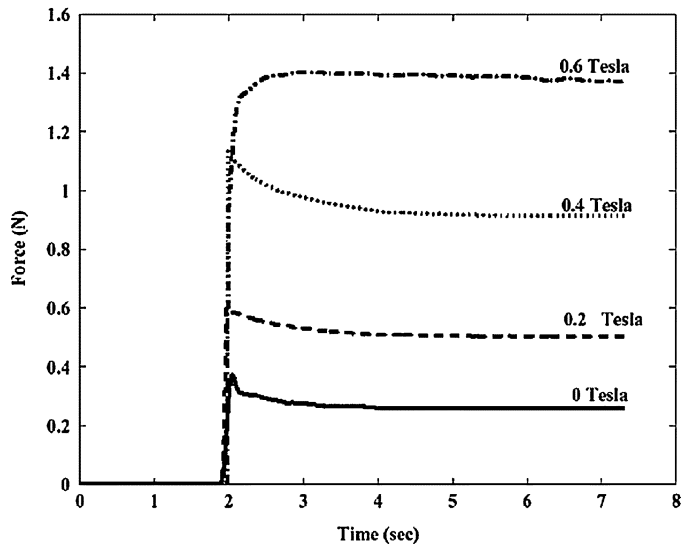


Fig. 7. MRF response to stepwise strain of 10% for increasing magnetic field up to saturation threshold.

over time down to a final steady value. As a matter of fact, a second-order Kelvin model has been chosen to describe the behavior of an MRF.

Such a model is composed of three springs (k_r, k_1 , and k_2) and two dampers (η_1 and η_2) and is mathematically described by the following differential equation of II order:

$$a_1 F(t) + a_2 \frac{d^2 F(t)}{dt^2} = b_0 \epsilon(t) + b_1 \frac{d\epsilon(t)}{dt} + b_2 \frac{d^2 \epsilon(t)}{dt^2}$$

where $F(t)$ is the input force, $\epsilon(t)$ is the output strain, and coefficients a_1, a_2, b_0, b_1, b_2 , and c_0 are a combination of the parameters $k_r, k_1, k_2, \eta_1, \eta_2$.

The accuracy between the MRF behavior and its model is estimated comparing the experimental and analytical stress relaxation curves. Fig. 8 reports the comparison between an experimental curve acquired from the MRF submitted to stepwise strain at a given magnetic field and the profile of the analytical curve obtained by the Kelvin model. It is worthwhile noting

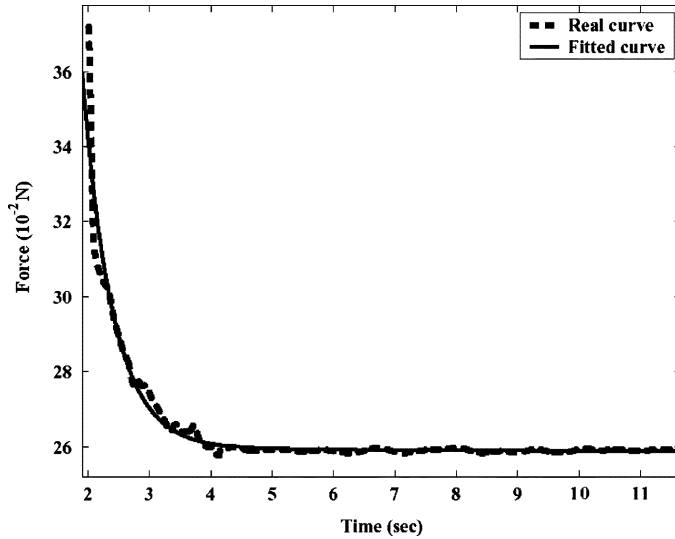


Fig. 8. Comparison between the experimental and analytical stress relaxation curve of the MRF (zoom view on relaxation part).

that the model reproduces the real MRF behavior with good agreement.

At this point, it is necessary to exploit the ability of the MRF to mimic real object softness. Since a possible field of application of the proposed haptic display could be minimally invasive surgery, the excited MRFs were compared with some biological tissues. Then, using the same methodology for MRFs, we performed a set of experiments based on stress relaxation tests on samples of biological tissue.

The stress relaxation curves for each biological tissue were compared with the output of the Kelvin model describing the MRF when excited by a proper magnetic field. In Fig. 9, for each couple of profiles, the higher curve is relative to stress relaxation acquired from biological tissue while the lower curve is relative to stress relaxation on the MRF. The initial and final values are very similar, while the relaxation times are different. In fact, biological tissues exhibit relaxation times greater than those relative to MRFs. Nevertheless, the general behavior is very similar and it is possible to affirm that with respect to the liver, spleen, and brain, a good agreement between the behavior of biological tissues and MRFs was attained. An experiment carried out using bone as the biological tissue provided unsatisfactory results. This is probably due to the fact that the magnetic field intensity needed to induce a compliance similar to these biological tissues is beyond saturation of the MRF used.

Furthermore, as preliminary work towards a haptic display based on MR fluid, a set of psychophysical tests were performed. A group of volunteers were asked to manipulate, using both hands at the same time, the biological tissue sample (chosen among brain, myocardium, spleen, liver, lower limb muscle, and lung) and the MR fluid specimen duly excited with magnetic field. Also, in this case, results regarding the brain, spleen and liver were very encouraging, while with respect to myocardium, lower limb muscle, and lung the analogy was not satisfactory. More details on such psychophysical results will be presented in a separate paper.

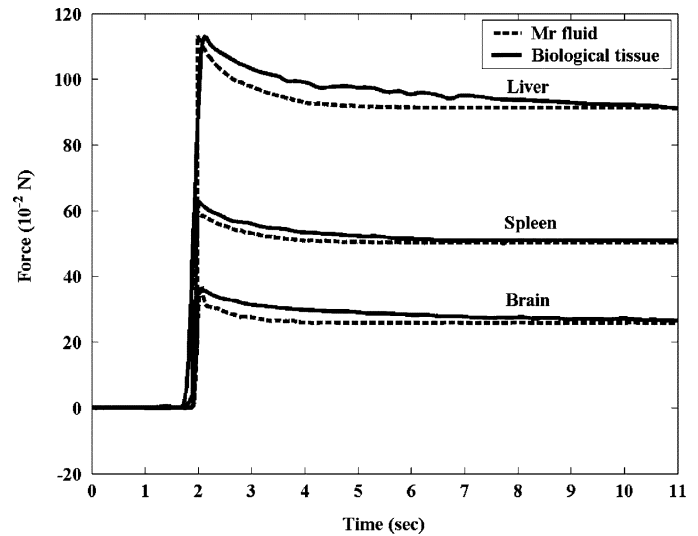


Fig. 9. Comparison between the stress relaxation curves of some biological tissues and the MRF.



Fig. 10. HBB-I prototype.

2) *The Second Prototype: The Haptic Black Box I (Hbb-I)*: To improve the test on the magnetorheological characteristics of the fluid and to try and obtain a better likeness between the excited fluid and different materials, a second laboratory-operating device was built. This new prototype of the immersive MRF-based display is shown in Fig. 10, and consists of a rectangular plastic box containing the MR fluid and a series of electrical coils to magnetically excite the fluid [41], [42]. Unlike the previous prototype, this device presents an easy accessibility to the fluid, and a 2-D excitation system.

A proper number of cylindrical ferromagnetic cores, arranged in a 4×4 array, are placed below a plastic box which has a square base of $18 \text{ cm} \times 18 \text{ cm}$ and a height of 4 cm. Each ferromagnetic core is equipped with an electrical coil of 305 A that supports a maximum dc current of about 10 A. The magnetic field obtained by tuning the current into each coil allows to materialize 2-D objects with a given shape and compliance in the fluid.

Since the prototype was designed using the above cited FE software, in Fig. 11 its FE model is shown. During the modeling phase, taking into account the presence of two symmetry planes, only $1/4$ of the problem can be modeled. Then, in order to verify the agreement between the numerical model and the built device, a first simulation was performed considering the device without the MRF. The system was excited feeding the

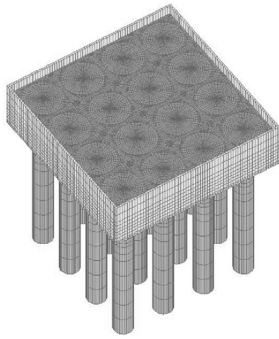


Fig. 11. The whole FE model of the HBB-I device.

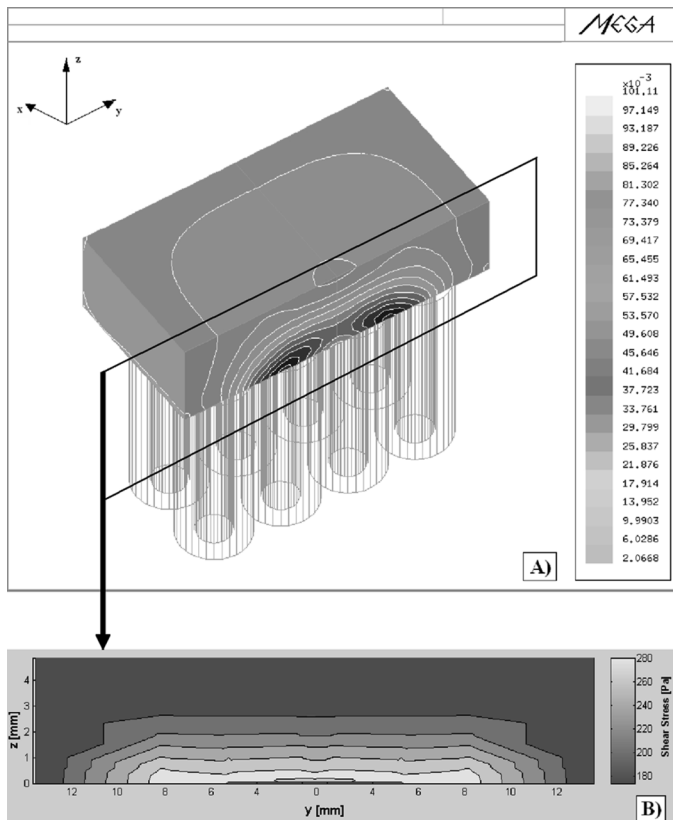


Fig. 12. Map of flux density B (Fig. A) and shear stress (Fig. B) in the HBB-I system.

eight centered coils with a constant electric current of 10 A, and a total number of about 24 000 AT. A portable Gaussmeter F.W. Bell/4048, equipped with an accurate Hall sensor, allows to measure the magnetic field in different points. The maximum percentage error is about 8%, showing a good agreement between the simulated field and the measured one.

Finally, the rheological behavior of the fully excited system, in the presence of MRF was simulated. The MR fluid has been modeled as a nonlinear material using the $B-H$ characteristic (Fig. 4) and the results in terms of magnetic field and shear stress are shown Fig. 12.

As it can be seen, the magnitude of B decreases as distance increases from the coil base and, at about 1 cm far from the box base, the field is reduced to about half. Unfortunately, this gradient of magnetic field induces a proportional decreasing of the shear strength, influencing the rheological behavior of the

MRF and smoothing the softness of the virtual object that could be perceived.

Besides the low values of magnetic field due to the absence of closed magnetic paths, another important HBB-I shortcomings is the impossibility of creating 3-D virtual objects which are constrained to lie on a plane.

However, these observations help us in defining some guidelines for a new advanced design capable of overcoming the 2-D limitation of the HBB-I prototype.

3) *Further Improvements: From a 2-D to a Quasi-3-D Device:* Although the results obtained by means of the previous prototypes were encouraging, currently the performance of these displays is quite poor, in part due to the 1-D or 2-D limitation of such devices. In particular, it is possible to report some general considerations on the main problems that have to be treated in the design of a new electromagnetic device capable of properly exciting a specified volume of MRF. A first critical point regards the paths of the magnetic flux that, as clearly shown by the HBB-I device [43], close themselves in air increasing the magnetic reluctance and, consequently, decrease the magnetic field inside the MRF. A second problem, instead, concerns the MRF characteristics. The relative permeability of such fluids is comparable to that of air, leading to a huge magnetic reluctance with a decrease of the magnetic field. Furthermore, both the ferromagnetic materials (the MRF and the iron of the cores) are highly nonlinear compromising the performance of the whole system. However, it is possible to introduce some solutions for the described problems. The reduction of the reluctance of the magnetic paths could be obtained introducing ferromagnetic yokes and cores to close the magnetic flux paths. The achievement of a suitable field spatial resolution could be made by increasing the number of ferromagnetic cores below the box containing the MRF. Then, concerning the relative permeability of the MRF, a compromise between an easy access to the fluid and the reduction of magnetic reluctance would allow for the identification of a proper size of the MRF volume to be energized. Finally, the problem of the saturation of the nonlinear ferromagnetic materials could be attenuated using special materials and increasing the transversal section of the ferromagnetic yokes and columns.

Taking into account such general considerations, two devices with improved performance in terms of magnetic field and its spatial resolution inside the MRF have been designed and simulated. The first of such new devices was described and analyzed by the authors in [44]. The second, named HBB-IMP and shown in Fig. 13, differs from the previous one in the augmented number of the ferromagnetic cores.

A first feature of the HBB-IMP is a new closed plastic box containing the MR fluid and equipped with a latex glove. An operator can insert his/her hand in the box in order to discriminate shapes and compliance of the virtual object suitably materialized by controlling the magnetic field in the MRF. A second characteristic is the presence of an external ferromagnetic system (structures 1, 2, and 3), and two subsystems (structure 4 with its twin 4'), composed of a series of ferromagnetic "pistons" symmetrically positioned with respect to the center of the plastic box. The usefulness of these two subsystems lies in their ability to dynamically address the magnetic flux in different regions of

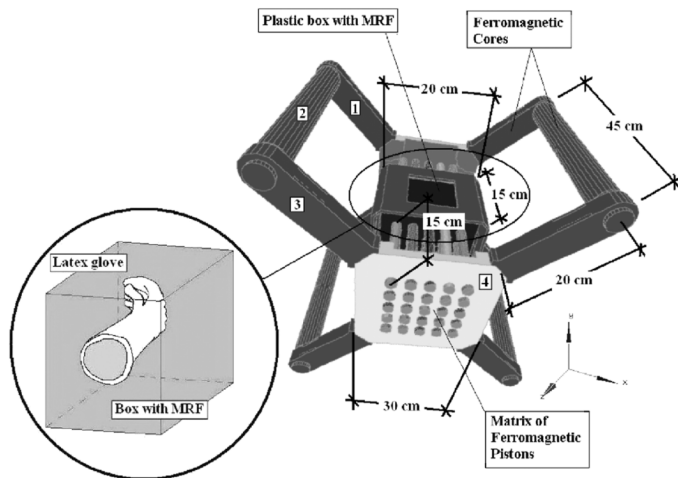


Fig. 13. Architecture and finite-element model of the second improved device: the HBB-IMP.

the MR fluid. As shown in Fig. 14, each piston, wound by an electrical coil for a fine control field resolution, can be moved along its axial direction. When all the pistons are at rest (far from the MRF), the reluctance of the magnetic path B-B' is very high and the value of flux density in the fluid is neglectable. On the contrary, when two opposed pistons are "in action," the air gap along the magnetic path A-A' is reduced resulting in an increase of magnetic flux in a specified volume of fluid corresponding to the x - y position of the pistons. Finally, a ferromagnetic sheet is placed around the plastic box capable of collecting a part of the leakage flux, increasing about three times the field spatial resolution inside the fluid.

Controlling the modulus and the spatial resolution of the magnetic field allows to reconstruct many objects of different shapes in the MRF. The magnetic field is tuned acting both electrically (varying the value of the current in some coils) and mechanically (moving the pistons).

The device was designed by means of the cited numerical code, using different values of dc current both in the main coils positioned around the external structure and in the coils around each ferromagnetic piston. The MR fluid was simulated as a nonlinear material using the B - H characteristic (Fig. 4). Then, due to the symmetry of the system, only 1/8 of the problem was modeled. Fig. 15 shows the flux density B along the line A-A' in the middle of the fluid, when only one couple of pistons are in action (center piston and its opposed). Fig. 16(A) shows the map of flux density B and its profile along the indicated line A-A' in

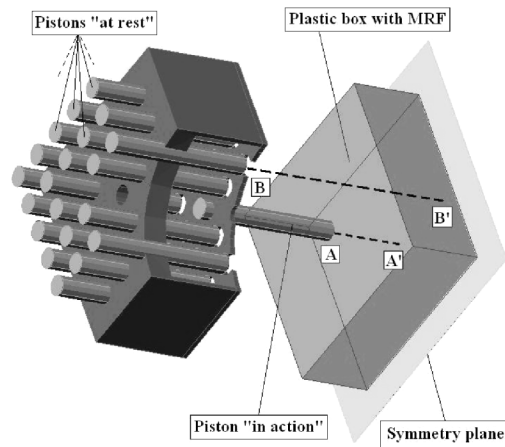


Fig. 14. System of ferromagnetic pistons to address the flux in the MRF.

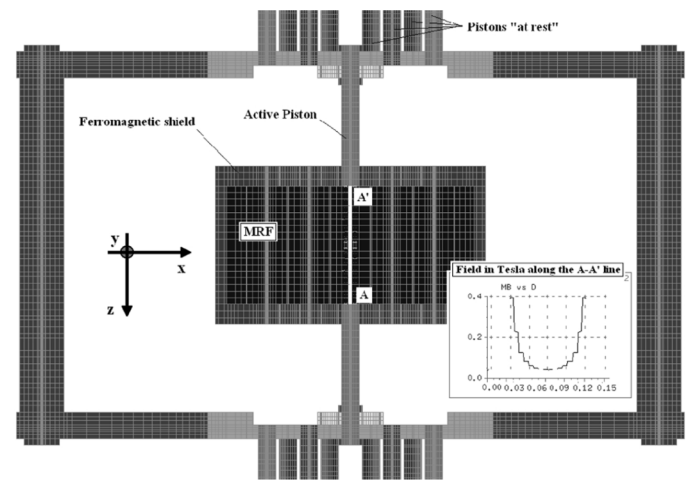


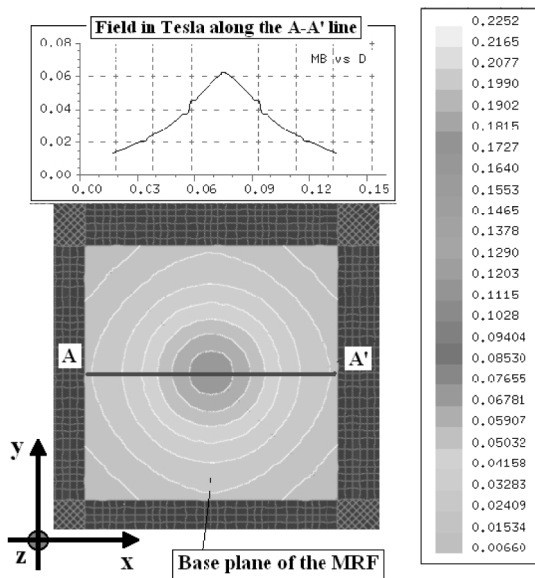
Fig. 15. Flux density B along the line A-A' when a couple of pistons are "in action."

the plane $z = 0$, when only one couple of pistons are in action (central piston and its opposed) and with the coil feed at their maximum permissible current.

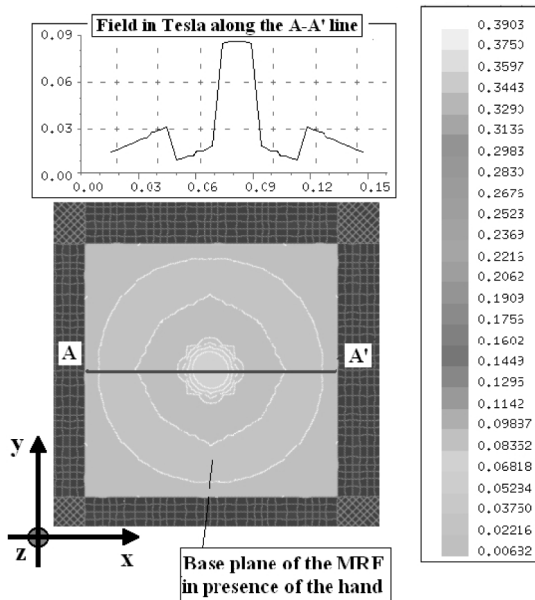
Fig. 16(B) shows the flux density B in the same condition as in Fig. 16, but with a hand inside the fluid (modeled setting to 1 the relative permeability of that volume). Fig. 17 shows the map of the flux density in the whole system.

Finally, in order to verify the improvement of this device in comparison with the HBB-I prototype, the flux density B for both devices has been compared. Fig. 18 shows the profiles of magnetic field simulated in the HBB-I and HBB-IMP devices along a line at a distance of about 10 mm from the box's base when four pistons (indicated with the black points in the figure) are equally energized. The increase of the magnetic field in the HBB-IMP is due to the presence of the mobile pistons that are able to address the flux in a specific region of the MRF.

Although from a magnetic point of view, the last two devices presented better performance in comparison with the previous HBB-I system, they were not built because the limitation in creating virtual objects with different shapes. In fact, the HBB-IMP device allows to materialize only some $2D + k$ objects inside the MRF, where the third dimension (k) is fixed and defined *a priori* by the height of the box containing the fluid.



A)



B)

Fig. 16. Flux density in the fluid at $z = 0$: (A) with only MRF in the box; (B) with a hand inside the fluid.

However, the obtained results have shown that the use of the mobile pistons to dynamically address the magnetic flux in the system increases the magnetic field and its spatial resolution inside the MRF. Furthermore, the simulation results have suggested the possibility of applying such a solution not only to the base of the plastic box but also to its lateral surface to improve the device performance. In such a way, by somehow controlling also the third dimension (k), the system could be led towards a quasi-3-D resolution.

III. A NEW ADVANCED QUASI-3-D PROTOTYPE: THE HAPTIC BLACK BOX II (HBB-II)

The models hereto described and simulated present a relevant shortcoming because they work only with a 1-D or 2-D

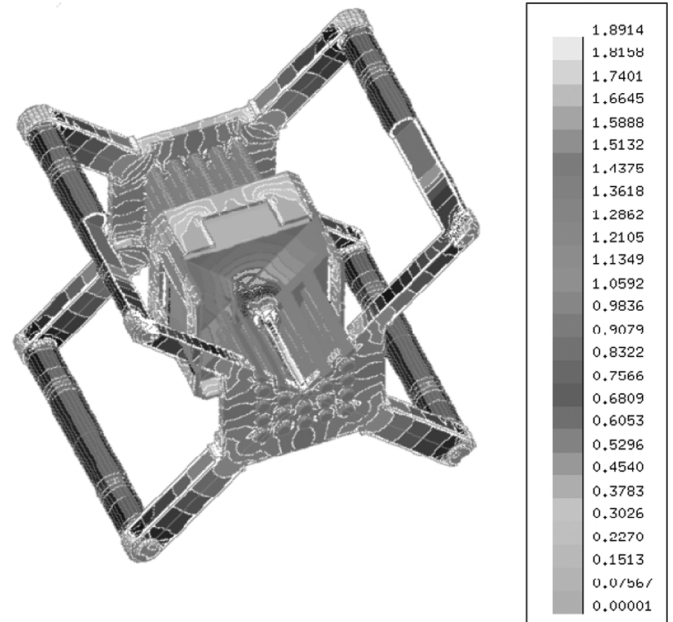


Fig. 17. Map of the flux density in the HBB-IMP device.

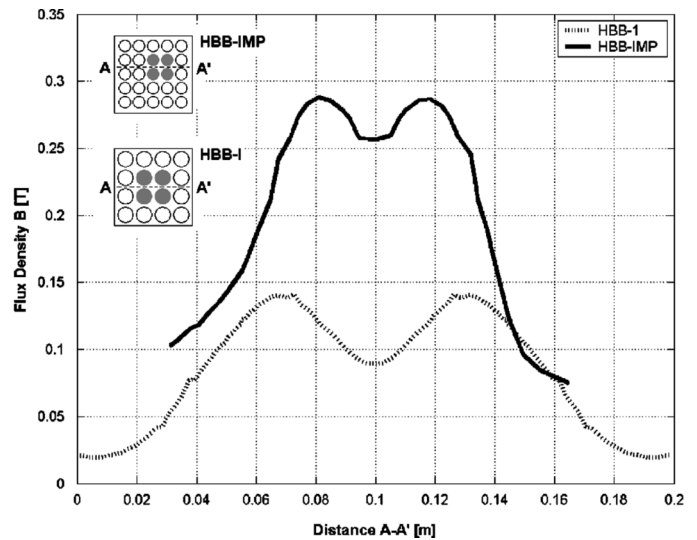


Fig. 18. Comparison between the flux density B along the line $A-A'$ in the HBB-I and HBB-IMP devices.

resolution linked to the $x-y$ axes of the MRF box, with x and y placed on the box's base. However, on the basis of the results obtained with the previous prototypes, a new advanced device towards quasi-3D free-hand exploration was designed and built. The novel device, named HBB-II, presents a cylindrical-shaped plastic box containing the MRF and a series of ferromagnetic cores, positioned around the plastic box and used to dynamically address the magnetic flux inside the fluid. A hand wearing a latex glove can be inserted into the cylindrical plastic box and can interact with the MRF perceiving and discriminating different virtual objects.

A. Detailed Description of the HBB-II

The architecture of this new 3-D display is reported in Fig. 19, where a schematic view of the device without coils is shown.

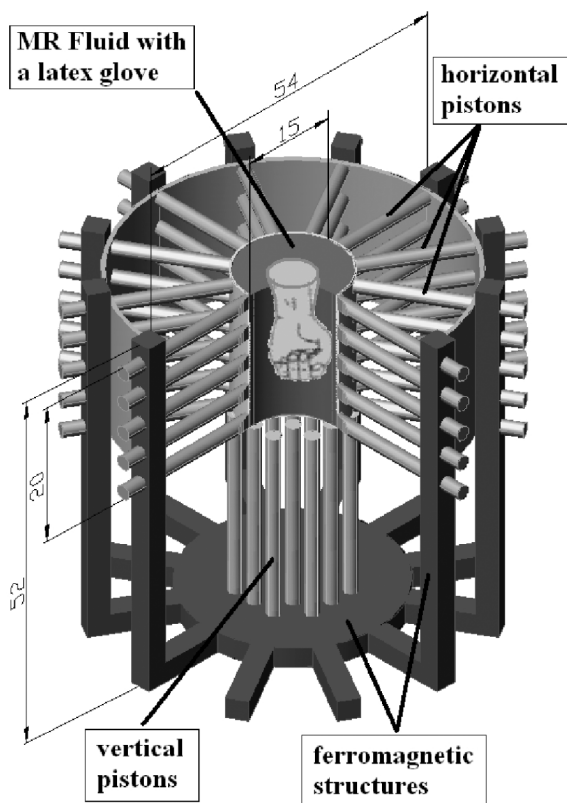


Fig. 19. Architecture of the new HBB-II device without coils (dimensions are in centimeters).

It is possible to decompose the whole system into four main parts.

- *The plastic box:* used to contain the MRF, it is cylindrically shaped to obtain a symmetrical system. The box is internally equipped with a latex glove to freely handle the fluid. Since the dimensions of the box have to respect a compromise between an easy accessibility to the fluid and a reduction of magnetic reluctance, it has a circular base with a diameter of about 15 cm and a height of about 50 cm.
- *The ferromagnetic structure:* used to close and to address the magnetic flux. It is composed of 10 vertical columns bolted to an iron circular plate and a series of 72 “pistons” free to move along the radial trajectory with respect to the plastic box containing the MRF. Twenty-two of such pistons are arranged in a circular matrix form below the box’s base; the remaining fifty, arranged in series of 10×5 are placed around the lateral surface of the plastic box. They are constrained to slide in special holes present in the superior part of each column. All the cores used are composed of ferromagnetic material AISI 1040 having enough magnetic permeability and suitable magnetic saturation-threshold to reduce the transversal sections. Then, taking into account such a saturation threshold, the iron plate has a diameter of 30 cm and a height of 1.5 cm. Each column has a base diameter of 4.5 cm and a height of 35 cm. Each piston, instead, has a base diameter of 2 cm and a height of 15 cm.

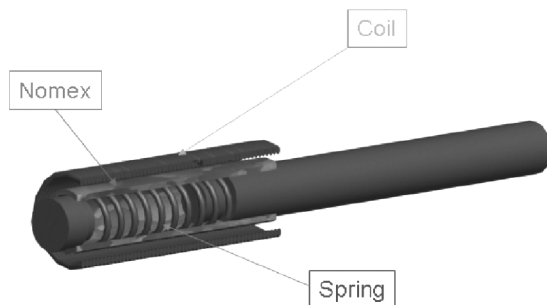


Fig. 20. Particular of secondary-coils system equipped with auxiliary system.

- *The coil system:* used to produce the proper magnetic field for the energization of the MRF. In the system, there are two types of coils. The first one, so-called *primary-coils*, is positioned around the inferior part of the columns and is used to create the main magnetic field. The second type, so-called *secondary-coils*, is positioned around the 72 pistons and is used either for the movement of the pistons themselves or for a fine control field resolution. Each primary-coil is built with about 5500 A of enamelled copper wire having a low thermal resistivity. They are arranged in 11 layers of 50 turns around a hollow plastic cylindrical support of an inner diameter of 46 mm and total length of 110 mm. The electric resistance of each primary-coil is 0.58Ω at 27°C . The secondary-coils consist, instead, of about 2700 A, arranged in five layers of 54 turns around a hollow plastic cylindrical support of an inner diameter of 21 mm and a total length of 150 mm. The electrical resistance of each secondary-coil is 0.1Ω at 27°C . All the coils are connected to an external electronic power system to obtain the desired magnetic field in different regions of the fluid.
- *The control system:* used to control the current in each coil for a double purpose. From an electrical point of view, it adjusts the value of current for a direct modulation of the magnetic field. From a mechanical point of view, the current in each coil allows to move the piston that is inserted into the plastic cylindrical support as in a classical solenoid with a plunger. When the coil is not electrically excited, a nonmagnetic aluminum spring keeps the piston in its initial position. A particular of the arrangement of the secondary coil system to activate the piston is shown in Fig. 20.

B. Operation of the Device

The HBB-II operates as follows. Let’s assume that we want to obtain a small hemisphere of MRF at the bottom of the box, or to create a cylinder of MRF with the axis along the radial direction at a given height of the plastic box. Once the choice of the MRF region to be energized by the magnetic field has been made, the corresponding pistons must be activated feeding the relative secondary-coils. Then, tuning the current in those primary and secondary coils belonging to the cores that compose the magnetic path, it is possible to change the rheology of the fluid and to obtain different compliance.

When the pistons are at rest (far from the plastic box), the reluctance of the magnetic path, closed along the $B - B'$ line (see

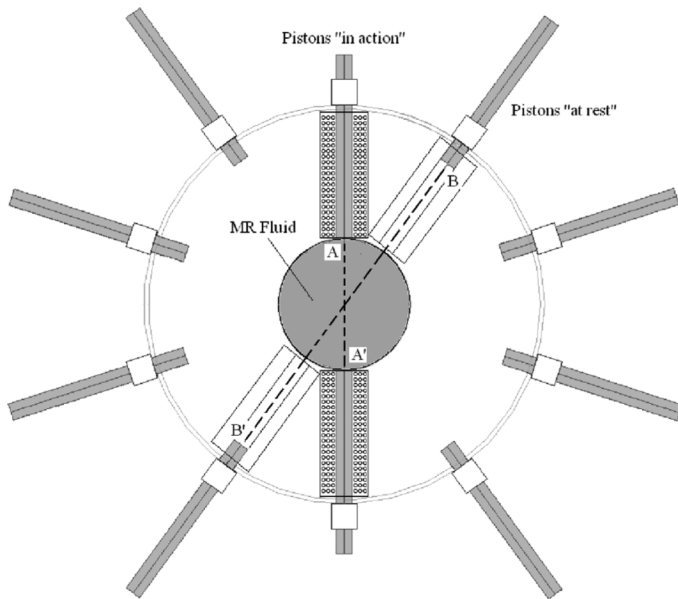


Fig. 21. Schematic view of the operation of the pistons of the HBB-II.

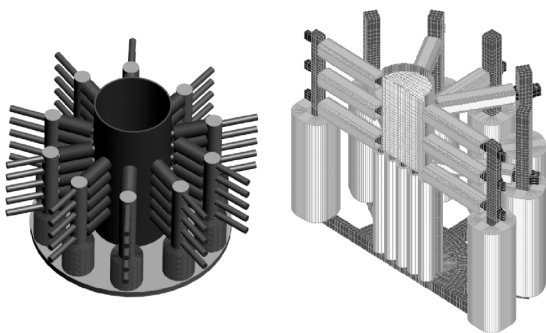


Fig. 22. Mechanical design of the HBB2 with coils and FE model.

Fig. 21), is very high resulting in a negligible value of magnetic flux in the fluid. On the contrary, when two or more pistons are “in action” (close to the plastic box), the gap along the magnetic path $A - A'$ is reduced implying an increase of magnetic flux in the corresponding MRF volume. In summary, the modulus of the magnetic field in a specified portion of the MRF and its spatial resolution can be controlled acting both electrically, varying the value of the current flowing into some coils, and mechanically, moving the pistons. In such a way, it is possible to reconstruct many objects of different shapes in different zones within the box containing the fluid.

C. FEM Analysis of the HBB-II

In the design phase, a set of numerical simulations with the use of the above cited 3-D finite-element code have been performed in order to verify and check the solution proposed to improve the performance of the HBB-II.

Fig. 22 shows the mechanical design of HBB-II with all the coils and the FE model used for the numerical simulation of the device. The obtained results are discussed below.

Fig. 23 shows the profile of the magnetic field B along the line $A-A'$ at a distance of about 10 mm from the box base when four pistons (indicated with the black points in the figure) below

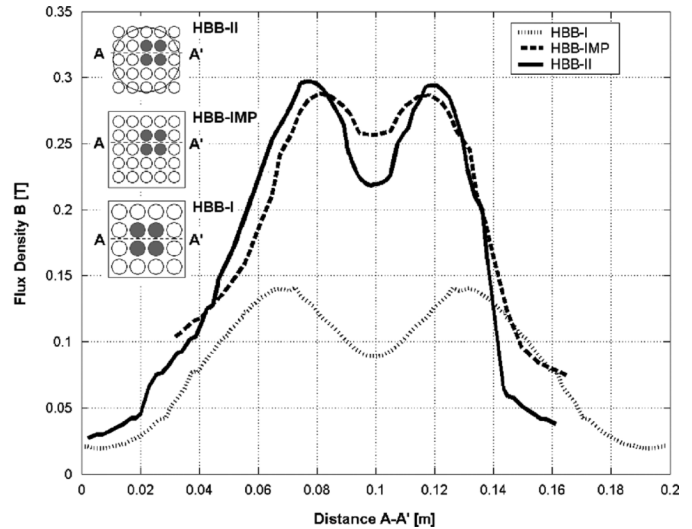


Fig. 23. Comparison between the flux density B along the line $A-A'$ in the HBB-I, HBB-IMP, and HBB-II devices.

the base are equally energized. It can be seen that the magnetic field inside the MRF almost has the same values in both the HBB-IMP and the HBB-II devices. However, the ability of this new device to control the movement of the mobile pistons allows to obtain various quasi-3-D virtual objects, showing more flexibility with respect to the HBB-IMP device.

Figs. 24–26 show some of the possible configurations that could be obtained with the HBB-II device. In particular, Fig. 24 shows the map of the flux density at the middle plane of the fluid when two opposite pistons operate and when the hand of an operator is inserted into the MRF. The same figure also reports the profiles of the magnetic field and of the shear stress along the line $A-A'$. In the absence of an applied magnetic field, or in case of its low value, the MRF exhibits a liquid-state behavior. With the increase of the magnetic field, instead, the fluid develops a precisely controllable shear stress that allows the fingers of a hand to perceive the softness and a variable compressional compliance of the energized specimen. Fig. 25 shows the map of the flux density at the middle plane of the fluid when all the pistons of that plane operate. Also, in this case, the profiles of the magnetic field and shear stress along the indicated circumference are reported. The fingers can perceive a little hemisphere on the lateral surface of the box in correspondence with each active mobile piston. Furthermore, in order to better verify the correspondence between the magnetic field and the object shapes in the fluid, two other configurations have been simulated. Then, by using the field-shear stress nonlinear function of Fig. 4, these shapes have been outlined in the MRF. Fig. 26 shows the maps of the flux density and of the shear stress when only the central vertical piston below the base of the fluid operates. As it can be seen, a hemisphere of given softness at the basis of the box should be perceived.

In Fig. 27 instead, the same maps are shown when a piston below the base and a piston on the lateral surface are in action. In this case, an L-shaped object is materialized inside the fluid. However, many other configurations could be envisaged and implemented, allowing to perceive different objects of desired shapes and compliance.

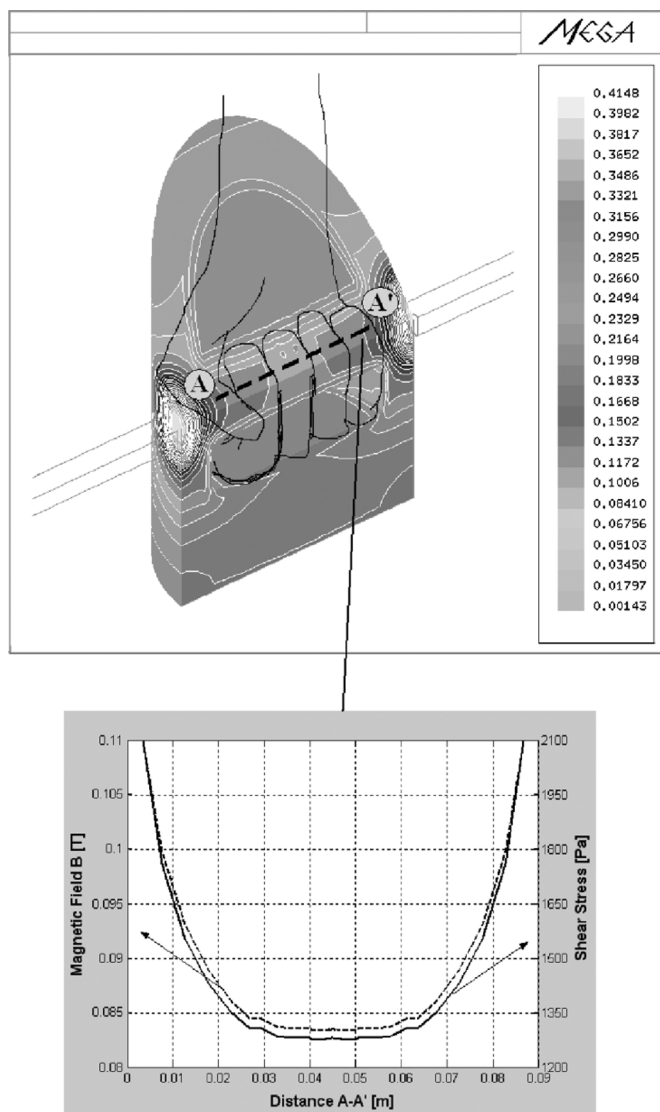


Fig. 24. Map of flux density in the HBB-II at the middle plane of the fluid when 2 opposite pistons operate and with a hand inside the MRF, and profile of flux density and shear stress along the line A-A'.

D. Prototype

As a result of the design phase, the HBB-II MRF-based display was built. In Fig. 28, a picture of the complete final prototype is shown. In order to verify the agreement between the FE model and the built device, a set of experimental measurements has been performed. Then, by using a portable Gaussmeter F.W. Bell/4048 equipped with an accurate Hall sensor, the magnetic fields were measured at the points indicated in Fig. 29. The results are reported in Table I, showing a good accuracy between the simulated field and the measured one. Furthermore, the haptic environment that controls the HBB-II was implemented by developing a tool in Visual C++ in order to decide and to impart the control strategy. The software was designed taking into account typical characteristics of a VE, including real-time and feedback control by means of a proper interface. The tool consists of a simple dialog based on graphical user interface (GUI). The core of the tool is a haptic thread which runs at 1 kHz and allows to fix the energization of the

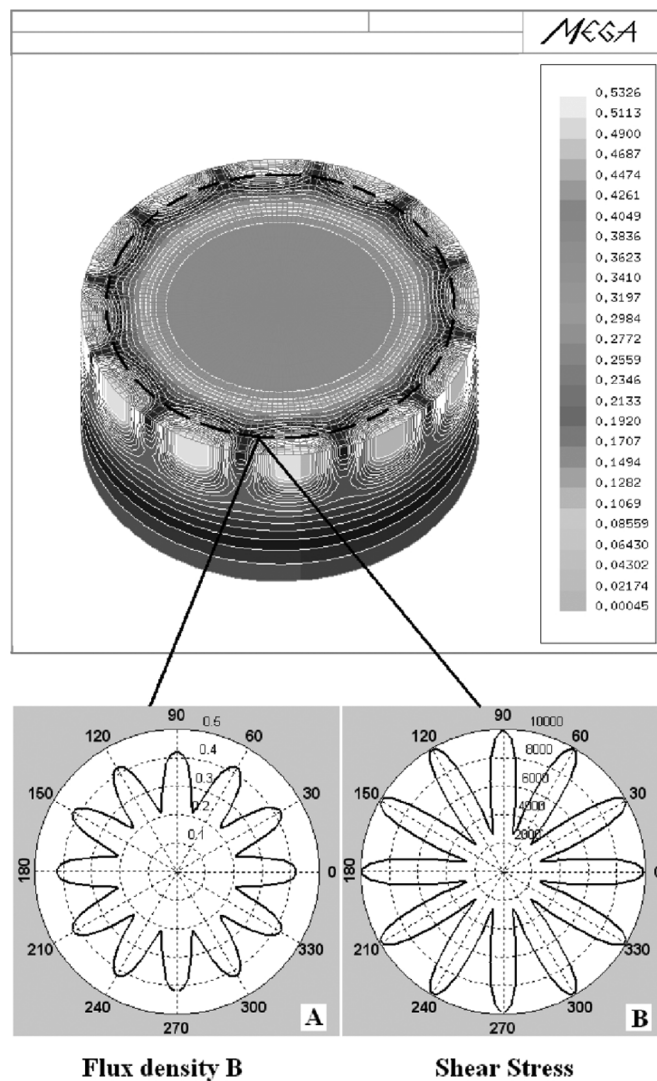


Fig. 25. Map of the flux density in the HBB-II at the middle plane of the fluid when all the pistons of the plane operate, and profile of the flux density and shear stress along the indicated line.

HBB-II device. By setting the run-time and the electric current in each coil and by using a virtual button on the GUI, it is possible to start and to stop the experimental session. In this case, a low-level control was implemented by the use of a real-time class in order to synchronize the movements with a 3-D Open GL simulation of the model and to realize the required haptic timing.

Finally, in Fig. 30, a view of the screenshot to control the operations of the device is shown.

This HBB-II prototype will be used to perform a set of psychophysical tests, whereby volunteers will be asked to analyze and verify the realism of the display in mimicking different object shapes and/or material characteristics.

IV. CONCLUSION AND FUTURE WORK

In this work, the results of a novel use of magnetorheological fluids for the development of innovative haptic interfaces have been presented. Several devices have been designed which include a controlled volume containing the fluid and a series

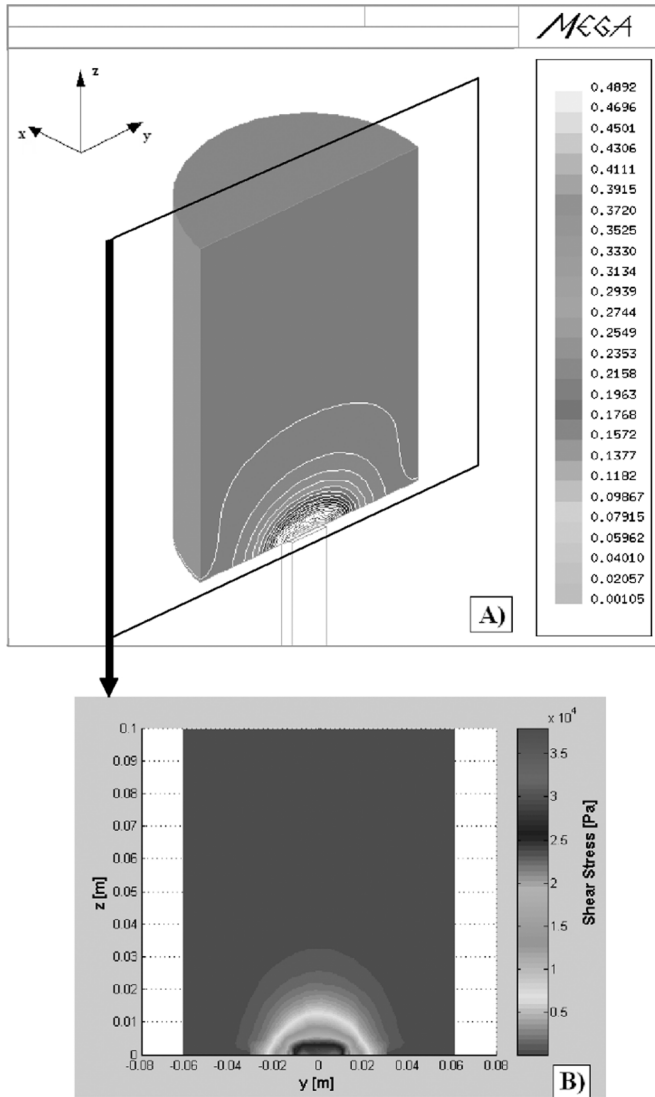


Fig. 26. Map of the flux density and shear stress in the HBB-II in the plane y - z when the central vertical piston on the base operates.

of ferromagnetic cores capable of addressing the magnetic field to a specified region of the MRF. In this way, the developed haptic display should guarantee an unconstrained manipulation of virtual objects. Starting from the design and construction of a first prototype (the Pinch Grasp) used to test the behavior of the MRF under the action of a controllable magnetic field, different electromagnetic devices have been designed, simulated, and analyzed. The results obtained during this phase have been used to build the last operating prototype, the HBB-II, capable of materializing some quasi-3-D virtual objects inside the fluid. The characteristics of the construction and the used materials have been shown in detail. The paper has been completed by the analysis of the performance in experimental measurements on the prototypes. Work is in progress following two lines of research. The first one regards the psychophysical tests on the final built prototype to verify the correspondence between some biological tissue samples and the MRF specimen duly excited with a controlled magnetic field. The second line of research concerns the optimization of the electromagnetic haptic display

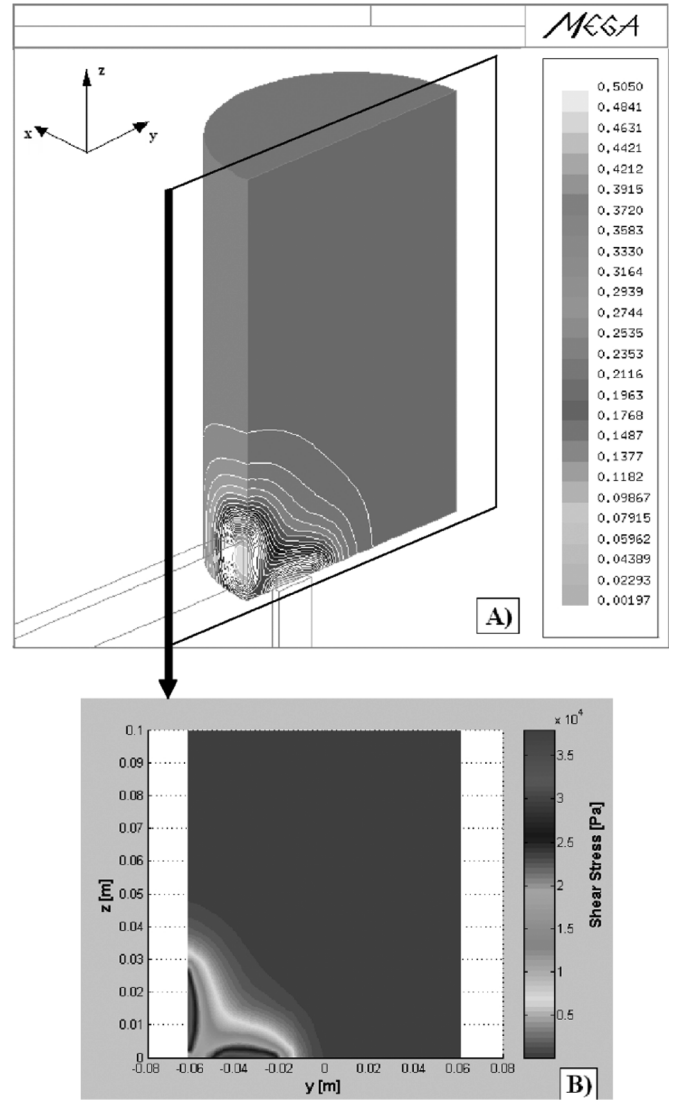


Fig. 27. Map of the flux density and shear stress in the HBB-II in the plane y - z when a piston below the base and a piston on the lateral surface operate.

to reduce its weight and to improve the spatial resolution of the magnetic field inside the MR fluid.

APPENDIX

A. Field Formulation in the Used FEM Software

For regions with no source current, the field formulation in the used FE code (MEGA), is expressed in terms of total magnetic scalar potential ψ

$$\begin{aligned}\mathbf{H} &= -\nabla\psi \\ \nabla \cdot (\mu\nabla\psi) &= 0.\end{aligned}$$

Using the “reduced scalar potential” formulation for the regions containing source current, it is possible to write

$$\mathbf{H} = -\nabla\phi + \mathbf{H}_s$$

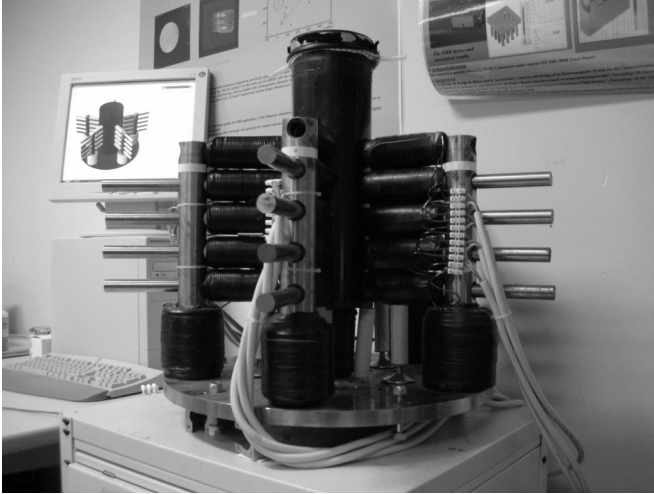


Fig. 28. HBB-II: picture of the final prototype.

TABLE I
COMPARISON BETWEEN FEA AND EXPERIMENTAL RESULTS

Points of measurements	Estimated \mathbf{B}	Measured \mathbf{B}	Error
1	0.12 T	0.1171 T	2.5%
2	0.027 T	0.0248 T	8.8%
3	0.017 T	0.016 T	6.2%
4	0.031 T	0.0290 T	6.9%
5	0.013 T	0.0123 T	5.7%
6	0.0096 T	0.0085 T	9.1%

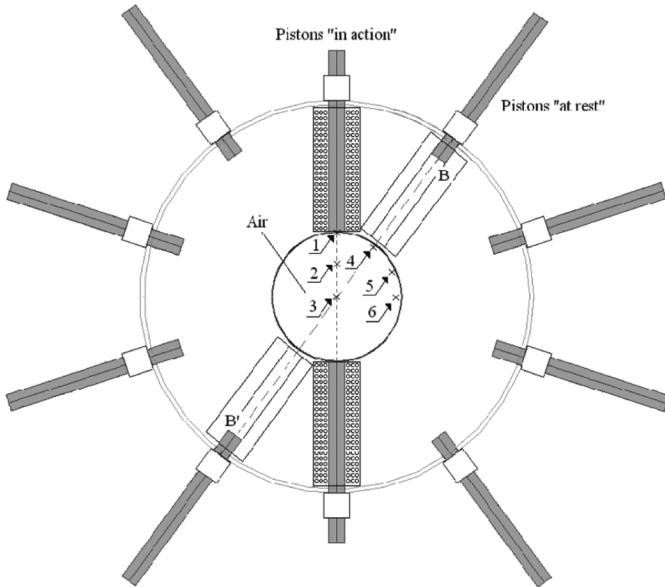


Fig. 29. Measurement points of flux density in the HBB-II without the MRF.

and consequently

$$-\nabla \cdot (\mu \nabla \psi) + \nabla \cdot (\mu \mathbf{H}_s) = 0$$

where μ is the nonlinear function of the B - H characteristics and \mathbf{H}_s is the field due to the source current calculated using

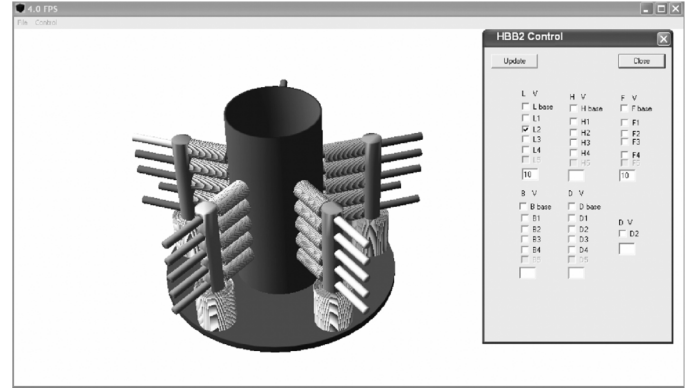


Fig. 30. HBB-II: Visual C++ GUI screenshot.

Biot-Savart law

$$\mathbf{H}_s = \frac{1}{4\pi} \int J \times \nabla \left(\frac{1}{r} \right) dV.$$

ACKNOWLEDGMENT

This work was supported in part by the European Commission under Contract IST-4-027141 Immersence.

REFERENCES

- [1] MEGA, "User Manual," Bath University, Nov. 2000.
- [2] A. Bicchi, E. P. Scilingo, D. Dente, and N. Sgambelluri, "Tactile flow and haptic discrimination of softness," in *Multi-Point Interaction with Real and Virtual Objects*, F. Barbagli, D. Prattichizzo, and K. Salisbury, Eds. New York: Springer-Verlag, 2005, pp. 165–176, number 18 in STAR—Springer Tracts in Advanced Robotics.
- [3] E. Ricciardi, N. Vanello, D. Dente, N. Sgambelluri, E. P. Scilingo, C. Gentili, L. Sani, V. Positano, F. M. Santarelli, M. Guazzelli, J. V. Haxby, L. Landini, A. Bicchi, and P. Pietrini, "Perception of visual and tactile flow activates common cortical areas in the human brain," in *Proc. EuroHaptics 2004*, Germany, Jun. 5–7, 2004, pp. 290–292.
- [4] N. Vanello, E. Ricciardi, D. Dente, N. Sgambelluri, E. P. Scilingo, C. Gentili, L. Sani, V. Positano, F. M. Santarelli, M. Guazzelli, J. V. Haxby, L. Landini, A. Bicchi, and P. Pietrini, "Perception of optic and tactile flow both activate V5/MT complex in the human brain," presented at the 10th Annu. Meeting of the Organization for Human Brain Mapping, 2004.
- [5] G. Ambrosi, A. Bicchi, D. De Rossi, and P. Scilingo, "The role of contact area spread rate in haptic discrimination of softness," in *Proc. IEEE Int. Conf. Robotics and Automation*, Detroit, MI, 1999, pp. 305–310.
- [6] J. D. Carlson, "The promise of controllable fluids," in *Proc. Actuator 94*, H. Borgmann and K. Lenz, Eds., AXON Technologies Consult GmbH, 1994, pp. 266–270.
- [7] J. D. Carlson, D. N. Catanzarite, and K. A. St Clair, "Commercial magneto-rheological fluid device," in *Proc. 5th Int. Conf. ER Fluids, MR Suspensions and Associated Technology*, W. Bullough, Ed. Singapore: World Scientific, 1996, pp. 20–28.
- [8] J. D. Carlson and K. D. Weiss, "A growing attraction to magnetic fluids," *Mach. Des.*, pp. 61–66, Aug. 1994.
- [9] C. W. Macosko, *Rheology: Principles, Measurements, and Applications*. New York: VCH, 1994.
- [10] W. I. Kordonsky, "Elements and devices based on magnetorheological effect," *J. Intell. Mater. Syst. Struct.*, vol. 4, no. 1, pp. 65–69, 1993.
- [11] K. D. Weiss *et al.*, "High strength magneto- and electro-rheological fluids," Society of Automotive Engineers, Tech. Paper 932451, 1993, pp. 425–430.
- [12] W. I. Kordonsky, "Magnetorheological effect as a base of new devices and technologies," *J. Magn. Magn. Mater.*, vol. 122, no. 1-3, pp. 395–398, 1993.
- [13] Z. P. Shulman, W. I. Kordonsky, and Zaitsgendler, "Structure, physical properties and dynamics of magnetorheological suspensions," *Int. J. Multiphase Flow*, vol. 12, no. 6, pp. 935–955, 1986.

- [14] A. M. Kabakov and A. I. Pabat, "Controlled magnetorheological shock absorbers," *Magnetohydrodynamics*, vol. 26, no. 2, pp. 222–227, 1990.
- [15] A. Savost'yanov, "Effects of magnetomechanical relaxation in a magnetorheological suspension," *Magnetohydrodynamics*, vol. 28, no. 1, pp. 42–47, 1992.
- [16] J. L. Spronston, L. C. Yanyo, J. D. Carlson, and A. K. El Wahed, "Controllable fluids in 2002—Status of ER and MR technology," in *8th Int. Conf. New Actuators & 2nd Int. Exhibition on Smart Actuators and Drive Systems*, Bremen, Germany, Jun. 10–12, 2002, pp. 333–338.
- [17] Delphi Automotive [Online]. Available: <http://www.delphiauto.com/pdf/chassispdfs/magneride.pdf> 2002
- [18] General Motors Corporation [Online]. Available: <http://www.cadillac.com/cadillacjsp/models/seville/ridecontrol.jsp>
- [19] C. D. Berg and P. E. Wellstead, "The application of a smart landing gear oleo incorporating electrorheological fluid," *J. Intell. Mater. Syst. Struct.*, vol. 9, no. 8, pp. 592–600, 1998.
- [20] S. B. Choi, Y. T. Choi, D. W. Park, and H. G. Lee, "Smart structures and integrated systems," in *Smart Structures and Materials*. San Diego, CA: SPIE (Int. Soc. Opt. Eng), 1998, vol. 3329, pp. 439–450.
- [21] J. P. Coulter, D. L. Don, M. Yalcintas, and P. J. Biermann, "Experimental investigation of electrorheological material based adaptive plate," *ASME Aerospace Division*, vol. 35, pp. 287–296, 1993.
- [22] K. H. Hagele, M. Engelsdorf, M. Mettner, M. Panther, N. Q. Tran, and E. Rubel, "Proceedings society of automotive engineers," in *Conf. Promise of New Technology in the Automotive Industry*, Torino, Italy, 1990, vol. II, pp. 37–46.
- [23] Z. Lou, R. D. Ervin, F. E. Filisko, and C. B. Winkler, "Electrorheologically controlled landing gear," *Aerospace Eng.*, vol. 13, no. 6, pp. 17–22, 1993.
- [24] A. Barbagli, A. Frisoli, K. Salisbury, and M. Bergamasco, "Simulating human fingers: A soft finger proxy model and algorithm," in *Proc. 12th Int. Symp. Haptic Interfaces for Virtual Environment and Teleoperator Systems HAPTICS*, 2004, pp. 9–17.
- [25] M. de Pascale, G. de Pascale, D. Prattichizzo, and F. Barbagli, "A new method for haptic gpu rendering of deformable objects," in *Proc. EuroHaptics 2004*, Munich, Germany, Jun. 5–7, 2004.
- [26] G. Bossis and E. Lemaire, "Yield stresses in magnetic suspensions," *J. Rheology*, vol. 35, pp. 1345–1354, 1991.
- [27] Y. Grasselli, G. Bossis, and E. Lemaire, "Field-induced structure in magnetorheological suspensions," *Progr. Colloid Polymer Sci.*, vol. 93, pp. 175–177, 1993.
- [28] E. Lemaire, Y. Grasselli, and G. Bossis, "Field induced structure in magneto and electro-rheological fluids," *J. Physique*, vol. 2, no. 3, pp. 359–369.
- [29] A. M. Kabakov and A. I. Pabat, "Development and investigation of control systems of magnetorheological damper," *Sov. Elect. Eng.*, vol. 61, no. 4, p. 55, 1999.
- [30] W. Kordonsky, O. Ashour, and C. A. Rogers, "Magnetorheological fluids: Materials, characterization, and devices," *J. Intell. Mater. Syst. Struct.*, pp. 123–130, 1996, 7.
- [31] V. A. Fedorov, "Features of experimental research into the characteristics of magnetorheological and electrorheological shock absorbers on special test stands," *Magnetohydrodynamics*, vol. 28, no. 1, pp. 96–98, 1992.
- [32] Y. Guozhi, M. Guang, and F. Tong, "The characteristics of electrorheological fluid and its application for vibration control," *J. Mach. Vib.*, vol. 4, pp. 232–240, 1995.
- [33] H. Böse, G. J. Monkman, H. Freimuth, H. Ermert, M. Baumann, S. Egersdörfer, and O. T. Bruhns, "ER fluid based haptic system for virtual reality," in *8th Int. Conf. New Actuators & 2nd Int. Exhibition on Smart Actuators and Drive Systems*, Bremen, Germany, Jun. 10–12, 2002, pp. 351–354.
- [34] G. Burdea and P. Coiffet, *Virtual Reality Technology*. New York: Wiley, 1994.
- [35] G. J. Monkman, "An electrorheological tactile display," in *Presence (Journal of Teleoperators and Virtual Environments)*. Cambridge, MA: MIT Press, Jul. 1992, vol. 1, pp. 219–228.
- [36] P. M. Taylor, D. M. Pollet, A. Hosseini-Sianaki, and C. J. Varley, "Advances in an electrorheological fluid based tactile array," *Displays*, vol. 18, pp. 135–141, 1998.
- [37] P. M. Taylor, A. Hosseini-Sianaki, and C. J. Varley, "Surface feedback for virtual environment systems using electrorheological fluids," *Int. J. Modern Phys. B*, vol. 10, no. 23& 24, pp. 3011–3018, 1996.
- [38] J. Fricke and H. Baehring, "Design of a tactile graphic I/O tablet and its integration into a personal computer system for blind users," in *Electronic Proc. 1994 EASI High Resolution Tactile Graphics Conf.* [Online]. Available: <http://www.rit.edu/easi/easisem/easisem tactile.html>
- [39] Y. Bar-Cohen, C. Mavroidis, M. Bouzit, B. Dolgin, D. L. Harm, G. E. Kopchok, and R. White, "Virtual reality robotic telesurgery simulations using MEMICA haptic system," in *Proc. SPIE 8th Annu. Int. Symp. Smart Structures and Materials*, Newport, CA, Mar. 5–8, 2001, Paper No. 4329-47 SPIE.
- [40] J. D. Carlson, "Portable Hand and Wrist Rehabilitation Device," U.S. Patent 6 117 093, Oct. 1998.
- [41] E. P. Scilingo, N. Sgambelluri, D. De Rossi, and A. Bicchi, "Towards a haptic black box: Magnetorheological fluid based display for softness and shape exploration," in *Proc. IEEE Int. Conf. Robot. and Autom. 2003*, Taipei, Taiwan, R.O.C., Sep. 2003, pp. 2412–2417.
- [42] A. Bicchi, E. P. Scilingo, N. Sgambelluri, and D. De Rossi, "Haptic interfaces based on magnetorheological fluids," in *Proc. 2nd Int. Conf. Eurohaptics*, Edinburgh, Jul. 2002, pp. 6–11.
- [43] E. P. Scilingo, N. Sgambelluri, D. De Rossi, and A. Bicchi, "Towards a haptic black box: Magnetorheological fluid based display for softness and shape discrimination," in *Proc. IEEE Int. Conf. Robotics and Automation 2003*, Taipei, Taiwan, R.O.C., Sep. 2003, pp. 2412–2417.
- [44] A. Bicchi, M. Raugi, R. Rizzo, and N. Sgambelluri, "Analysis and design of an electromagnetic system for the characterization of magneto-rheological fluids for haptic interfaces," *IEEE Trans. Magn.*, vol. 41, no. 5, pp. 1876–1879, May 2005.

Manuscript received October 27, 2006; revised April 30, 2007. Corresponding author: R. Rizzo (e-mail: rocco.rizzo@dsae.unipi.it).

Rocco Rizzo received the Ph.D. degree in electrical engineering from the Department of Electrical Systems and Automation, University of Pisa, Pisa, Italy, in 2002.

He is Assistant Professor of Electrical Engineering at the University of Pisa. His primary area of research is focused on the development of analytical and numerical methods for the analysis of electromagnetic fields in linear and nonlinear media, applied to the design of electromagnetic devices for special purposes. He has published more than 30 papers in international journals and refereed conferences.

Dr. Rizzo is a member of the Academy of Nonlinear Sciences (ANS), Russia.

Nicola Sgambelluri received the Laurea degree in electronic engineering from the University of Pisa, Pisa, Italy, in 2001 and the Ph.D. degree in automation, robotics and bioengineering from the Department of Electrical Systems and Automation, University of Pisa, in 2006.

Currently he works at the Interdepartment Research Centre "E. Piaggio." His main research interests concern haptics, robotics, automation, bioengineering, electronics, and embedded control systems. He is author of several papers, contributions to international conferences, and chapters in international books.

Enzo Pasquale Scilingo graduated from the University of Pisa, Pisa, Italy, in 1995 and received the Ph.D. degree in bioengineering from the University of Milan, Milan, Italy, in 1998.

He is Assistant Professor of Bioengineering at the University of Pisa. His main research interests are in haptic interfaces, control, and instrumentation; biomedical and biomechanical signal processing, modeling; and wearable systems for telemonitoring. He has published more than 50 papers in international journals, books, and refereed conferences. He currently pursues his research activity at the Interdepartmental Research Center "E. Piaggio," University of Pisa.

Marco Raugi received the degree in electronic engineering from the University of Pisa, Pisa, Italy, in 1985 and the Ph.D. degree in electrical engineering from the Department of Electrical Systems and Automation, University of Pisa, in 1990.

He is currently a Full Professor of Electrical Engineering at the University of Pisa. His research activity is in the numerical methods for the analysis of electromagnetic fields in linear and nonlinear media. Main applications have been devoted to nondestructive testing, electromagnetic compatibility in transmission lines, and electromagnetic launchers. He is author of about 100 papers in international journals and conferences. He was general chairman of the ISPLC (International Symposium on PowerLine Communications) in March

2007 in Pisa and he has been the general chairman of the international conference PIERS (Progress In Electromagnetic Research Symposium) in March 2004 in Pisa. In the mainframe of international conferences (ACES, COMPUMAG, CEFC, ISPLC, PIERS) he served as chairman, session organizer, author of invited lectures, instructor of courses and tutorials, member or chairman of editorial boards.

Prof. Raugi was the recipient of the IEEE-IndustryApplication Society 2002 Melcher Prize Paper Award

Antonio Bicchi (S'87–M'89–SM'99–F'02) graduated from the University of Bologna, Bologna, Italy, in 1988 and was a postdoc scholar at Massachusetts Institute of Technology A.I. Lab in 1988–1990.

He is Professor of Automatic Control and Robotics at the University of Pisa, Pisa, Italy. His main research interests are in dynamics, kinematics, and control of complex mechanical systems, including robots, autonomous vehicles, and automotive systems; haptics and dextrous manipulation; theory and control of nonlinear systems, in particular hybrid (logic/dynamic, symbol/signal) systems. He has published more than 200 papers in international journals, books, and refereed conferences. He currently serves as the Director of the Interdepartmental Research Center “E. Piaggio” of the University of Pisa, where he has been leading the Automation and Robotics group since 1990.

Prof. Bicchi is Vice President of the IEEE Robotics and Automation Society for Member Activities. He has served IEEE and other professional societies, as well as several scientific journals, in many different capacities.